Preparation and Release Study of Ibuprofen-Loaded Porous Matrices of a Biodegradable Poly(ester amide) Derived from L-Alanine Units

Luis J. del Valle, Diana Roca, Lourdes Franco, Jordi Puiggalí, Alfonso Rodríguez-Galán

Departament d'Enginyeria Química, Universitat Politècnica de Catalunya, Avinguda Diagonal 647, E-08028, Barcelona, Spain

Received 12 June 2010; accepted 21 December 2010
DOI 10.1002/app.34017
Published online 13 June 2011 in Wiley Online Library (wileyonlinelibrary.com).

ABSTRACT: Scaffolds of a biodegradable poly(ester amide) constituted of L-alanine, sebacic acid, and 1,12-dodecanediol units (abbreviated as PADAS) were prepared by the compression-molding/particulate-leaching method. The influence of the type, size, and percentage of salt on the scaffold porosity and morphology was evaluated. The thermal behavior and crystallinity were also studied for samples obtained under different processing conditions. PADAS scaffolds were not cytotoxic because they showed good cell viability and supported cell growth at a similar ratio to that observed for the biocompatible materials used as a reference. The use of PADAS scaffolds as a drug-delivery system was also evaluated by the employment of ibuprofen, a drug with well known anti-inflammatory effects. Different drug-loading methods were considered, and their influence on the release in a Sörensen's medium was evaluated as well as the influence of the scaffold morphology. A sustained release of ibuprofen could be attained without the production of a negative effect on the cell viability. The release kinetics of samples loaded before melt processing was well described by the combined Higuchi/first-order model. This allowed the estimation of the diffusion coefficients, which ranged between 3×10^{-14} and 5×10^{-13} m^2/s. Samples loaded by immersion in ibuprofen solutions showed a rapid release that could be delayed by the addition of polycaprolactone to the immersion medium (i.e., the release rate decreased from 0.027 to 0.015 h^{-1}). © 2011 Wiley Periodicals, Inc. J Appl Polym Sci 122: 1953–1967, 2011

Key words: biocompatibility; biological applications of polymers; drug delivery systems

INTRODUCTION

Tissue engineering techniques generally require the use of degradable porous scaffolds, which initially serve as a three-dimensional template for cell attachment and proliferation, and finally lead to tissue regeneration.[1] Considerable effort is being made to increase the range of available materials and improve scaffold structure because several restrictive functions must be accomplished.[2–12] Thus, optimal materials must balance their temporary mechanical properties with the desired degradation profile. Furthermore, materials must be biocompatible and nontoxic and have appropriate surface properties for cell attachment, proliferation, and differentiation.[13–15] Scaffolds should have a structure suitable for cell growth, support growing tissue, and allow the transport of nutrients and waste products to and from cells that are in charge of rebuilding new tissue. These requirements may be met mainly by the control of the degree of interconnectivity between pores of the right size. Finally, scaffold materials must be easily processed into a variety of shapes and sizes and produced at low cost and on a large scale.[16]

Several methods have been proposed to prepare porous scaffolds, as none of them is devoid of drawbacks.[17] Among these methodologies, we can find solvent casting/particulate leaching,[18,19] melt-based procedures (compression molding/particulate leaching,[20,21] injection molding and extrusion with blowing agents[22,23]), gas foaming,[24] supercritical CO_2,[25] phase separation,[26–29] fiber bonding,[30] microsphere sintering,[31] electrospinning,[32,33] *in situ* polymerization,[34] and rapid prototyping.[35] The first is the most commonly used because of its simplicity and the ability to control the pore size and porosity through the particle/polymer ratio and the particle size.

Implantation of engineered biomaterials might cause local inflammation because of the host's immune response;[36] thereby, they require the use of anti-inflammatory agents, whether steroidal or nonsteroidal. Within the last group, ibuprofen [2-(*p*-isobutylphenyl)propionic

Correspondence to: J. Puiggalí (jordi.puiggali@upc.es).
Contract grant sponsor: Ministerio de Ciencia y Tecnología (MICYT)/Fondo Europeo para el Desarrollo Regional (FEDER).
Contract grant sponsor: Agència de Gestió d'Ajuts Universitaris i de Recerca (AGAUR); contract grant numbers: MAT2009-11503, 2009SGR-1208.

a)

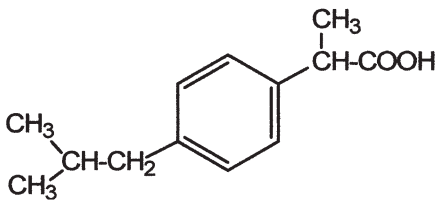

IBUPROFEN

b)

PADAS

Scheme 1 Chemical structures of (a) ibuprofen and (b) PADAS.

acid, Scheme 1(a)] has been widely used orally, intravenously, and even topically, for example, in postoperative conditions where an immediately available dose might be useful or required.[37–40] However, only recently have specific studies on ibuprofen loading into and release from porous scaffolds been reported.[41] In general, several aspects remain unstudied, for example, drug solubility, amount of loaded drug available for release, drug diffusion through the polymer matrix, and degradation and erosion mechanisms of the polymer.

Most biodegradable polymeric materials investigated for scaffold applications have already been employed as bioresorbable sutures (e.g., natural collagen and polyesters based on lactide, glycolide, and/or caprolactone[42–46]). Polysaccharides such as chitosan and glycosaminoglycans (e.g., hyaluronic acid[47]) have also been extensively considered. Polymers derived from naturally occurring monomers should generally be preferred materials for biomedical applications because their degradation products are nontoxic and can be well metabolized by the organism.

Poly(ester amide)s now constitute a promising family of biodegradable polymers for biomedical uses because of their combination of a degradable character, which results from the existence of hydrolizable ester groups (—COO—), with relatively good thermal and mechanical properties afforded by strong intermolecular hydrogen-bond interactions established between their amide groups (—NHCO—). Furthermore, they can be synthesized by several chemical methods to obtain polymers with segmented, random, and regular distributions.[48,49] In this way, these materials may cover a wide range of properties because of their flexible chemical composition and molecular microstructure.[48–50]

Different studies have focused on the use of poly(ester amide)s as viable biomaterials for tissue engineering applications (e.g., vascular grafts,[51] elastomeric materials[52,53]). Specifically, poly(ester amide)s that incorporate α-amino acid units have been extensively developed because, in general, they have been revealed to be biodegradable and biocompatible, and in addition, their mechanical, thermal, and degradation properties can be tuned by changes in their methylene/amide ratio.[54]

The polymer constituted of alanine, 1,12-dodecanediol, and sebacic acid units [PADAS, Scheme 1(b)] has also received attention because it can be easily obtained by a simple procedure based on an interfacial polymerization[55] and has good solubility and promising properties.[55–57] This work deals with the preparation of PADAS scaffolds by different procedures, their physical characterization, and the evaluation of their biocompatibility and capability of favoring cell ingrowth. The work also considers the application of PADAS scaffolds as drug-delivery systems. Thus, the release of ibuprofen, a hydrophilic drug with a well known pharmacologic effect, was evaluated; we took into account the scaffold morphology and the loading method.

EXPERIMENTAL

Materials

PADAS was synthesized, as previously described,[55] by the interfacial polycondensation of sebacoyl dichloride and the *p*-toluenesulfonic salt of bis(L-alanine)-1,12-dodecamethylene diester with carbon tetrachloride as an organic solvent and sodium carbonate as a proton acceptor. The weight-average molecular weight (M_w) and polydispersity index, estimated by gel permeation chromatography with poly(methyl methacrylate) standards, were 19,000 g/mol and 2.71, respectively.

The reagents for synthesis, polycaprolactone (PCL; M_w = 65,000 g/mol), ibuprofen, salts, and solvents were purchased from Aldrich (St. Louis, MO, USA) and were used as received. All reagents and labware for cell culturing were purchased from Sigma-Aldrich. MDCK cells (epithelial-like cells derived from Madin–Darby canine kidney) were purchased from ATCC (Manassas, VA, USA).

Sörensen's buffer (pH 7.4) was prepared by the dissolution of $Na_2HPO_4{\cdot}12H_2O$ (12.968 g) and KH_2PO_4 (1.796 g) in distilled water (1 L). The buffer contained 0.01% (w/v) of NaN_3 to prevent bacterial growth.

Preparation of scaffolds

PADAS disks with and without the selected porogen inorganic salt were prepared with a conventional Specac press. The applied pressure was always close to 3 bar. The charged mold was previously preheated at the appropriate temperature (105°C for

PADAS or its mixture with NaCl) or used at room temperature (PADAS mixture with NH_4HCO_3). After reorganization of the polymer, the composite material was removed from the mold, cooled if necessary, and soaked in water to leach out NaCl (48 h with renewal of water every 6 h) or NH_4HCO_3 (2 h at 45°C) particles.

NaCl and NH_4HCO_3 particles were previously sieved into micrometric fractions of 500 or 250 μm (BS, big size fraction) and 250 or 100 μm (LS, low size fraction).

Ibuprofen loading

Homogeneous PADAS/ibuprofen mixtures were prepared by the evaporation of dichloromethane solutions of the appropriate ratio of the two components. Porogen inorganic salt was then added to the PADAS/ibuprofen mixtures before the preparation of disks under a pressure of 3 bars and at a temperature of 105°C (PADAS or PADAS–NaCl mixtures with an ibuprofen load lower than 23%), 80°C (PADAS or PADAS–NaCl mixtures with an ibuprofen load equal or higher than 23%), and 25°C (PADAS–NH_4HCO_3 mixtures). The initial weight percentages of ibuprofen or the porogen agent always refer to the mixture of the specific compound with PADAS. Changes in the molding temperature were made to prevent decomposition of the NH_4HCO_3 salt or the plasticizing effect of ibuprofen, which requires a lower processing temperature at high concentrations. Disks were removed from the mold, cooled if necessary, and soaked in water to leach out the porogen agent, as indicated previously.

Alternatively, ibuprofen was loaded by the immersion of porous disks in ethyl acetate solutions containing different percentages of ibuprofen (2.5–5% w/v) and PCL (0–5% w/v) for 2 h.

Measurements of the physical properties and scaffold structures

Calorimetric data were obtained by differential scanning calorimetry with a TA Instruments Q100 series instrument equipped with a refrigerated cooling system, which operated from −90 to 550°C. Experiments were conducted under a flow of dry nitrogen with a sample weight of approximately 10 mg, whereas calibration was performed with indium. Heating and cooling runs were undertaken at a rate of 20°C/min.

Wide-angle X-ray diffraction (WAXD) patterns were taken at the CRG beamline (BM16) of the European Synchrotron Radiation Facility of Grenoble. The beam was monochromatized to a wavelength of 0.098 nm. Polymer samples were confined between Kapton films. The WAXD detector was calibrated with diffractions of a standard of an alumina (Al_2O_3) sample. The diffraction profiles were normalized to the beam intensity and corrected with consideration of the empty sample background. Deconvolution of the WAXD peaks was performed with the PeakFit v4 program by Jandel Scientific Software with Gaussian peak profiles assumed.

The structure of the porous scaffolds was evaluated by optical microscopy with a Zeiss Axioskop 40 Pol microscope equipped with a Zeiss AxiosCam MRC5 digital camera and scanning electron microscopy (SEM) with a JEOL JSM-6400 instrument. Gold coating was accomplished with a Balzers SCD-004 sputter coater.

The apparent density of the scaffolds ($\rho_{scaffold}$) was determined from the mass of the disk samples, and the volume was calculated from the thickness and diameter size. Porosity was estimated by division of the apparent density of the scaffolds by that of the polymer matrix (ρ_{pol}), which ranged between 1.16 and 1.10 g/mL, depending on the preparation conditions:

$$\text{Porosity}(\%) = [1 - (\rho_{scaffold}/\rho_{pol})] \quad (1)$$

The porosity and pore size distribution were determined for selected samples with an Autopore IV 9500 V1.07 mercury intrusion porosimeter (Micrometrics).

Cell adhesion and proliferation test

The MDCK cellular line was chosen as an appropriate system for evaluating the cell attachment and proliferation onto the scaffolds because of its characteristic growth as a monolayer, which allows it to colonize the material surface. MDCK cells were cultured in Dulbecco's modified Eagle medium supplemented with 10% fetal bovine serum, 50 U/mL penicillin, 50 μg/mL streptomycin, and 2 mM L-glutamine at 37°C in a humidified atmosphere with 5% CO_2 and 95% air. The culture medium was changed every 2 days, and for subculturing, the cell monolayers were rinsed with phosphate buffer saline (PBS) and detached by incubation with trypsin–ethylene diamine tetraacetic acid (0.25%) for 2–5 min at 37°C. The cell concentration was established by count with a Neubauer camera with 4% vital Trypan blue staining. The resulting cell suspensions (viability $\geq$ 95%) were then seeded separately onto the scaffolds.

PADAS disk scaffolds with a diameter of 1.3 cm and prepared from 60% NaCl low-size particles (LS fraction) with or without ibuprofen load (9%) were placed onto a 24-well culture plate, or tissue culture polystyrene (TCPS), and sterilized by UV irradiation for 15 min. Culture medium (1 mL) was added to each well, and the plate was incubated under culture conditions for 24 h to equilibrate the material. Then,

the medium was aspirated, and the materials were tested for cell adhesion and proliferation by exposure of the cells to direct contact with the material surface.

Cell adhesion assays were carried out by deposition of aliquots of 100 μL containing 5×10^4 cells onto the scaffolds. The cells were allowed to attach to the scaffolds in an incubator for 60 min. Then, 1 mL of culture medium was added to each well, and the culture was maintained for 24 h. Finally, each well was rinsed with PBS, and the number of attached cells was quantified by the 3-(4,5-dimethylthiazol-2-yl)-2,5-diphenyl-2H-tetrazolium bromide (MTT) assay (as described next).

We carried out the cell proliferation assays by seeding 2×10^4 cells onto the scaffolds. A lower cell number was used for the proliferation studies as compared with the adhesion studies to enhance the accessible area for cell proliferation to prevent confluence conditions from being reached in a short period of time. The assay was performed in a similar way to the adhesion assay, but the cells were allowed to proliferate for a longer time (i.e., 7 days). Then, the number of attached cells was again determined by the MTT assay.

The colorimetric MTT assay determines the cell viability by measurement of the absorbance at 540 nm. Briefly, the material was rinsed with PBS and then incubated with 1 mL of culture medium and 50 μL of MTT reagent (3 mg/mL MTT in PBS) for 4 h. Finally, the material was placed in a clean well, where the formazan dye produced by viable cells was solubilized in dimethyl sulfoxide to measure its absorbance.

We performed the adhesion and proliferation controls by culturing cells on the surface of TCPS, Thermanox (glass), and PCL. All attachment and proliferation measurements were normalized to the surface unit (cm^2). Five replicates for each experiment were averaged and graphically represented. One-way analysis of variance and Student t test were used to assess statistical significance ($p < 0.05$).

For microscopy observations, polymer disks were fixed in 2.5% glutaraldehyde–PBS overnight at 4°C, dehydrated by washing in an alcohol battery (30, 50, 70, 90, 95, and 100°) at 4°C for 30 min per wash, and finally, kept at 4°C.

The samples were dried on filter paper. To improve the contrast of cells adhered to the polymer surface, samples were dyed with Giemsa 2% for 5–10 min. Excess of dye was removed by washing in alcohol (70°). Finally, the samples were again dried on filter paper, mounted with Permount (Sigma-Aldrich) and analyzed with the optical microscope (Zeiss Axioskop 40 Pol microscope equipped with a Zeiss AxiosCam MRC5 digital camera). The dehydrated material was processed for SEM by a sputtering with carbon and observed with an Neon40 model scanning electron microscope (Zeiss).

Release experiments

Controlled release measurements were made with disks with a diameter of 1.3 cm. They were weighed and incubated at 37°C in an orbital shaker at 60 rpm in vessels with 100 mL of Sörensen's release medium (pH 7.4). The ibuprofen concentration in the release medium was evaluated by UV spectroscopy with a Shimadzu UVmini-1240 model. Calibration curves were obtained by the plotting of the absorbance measured at 263 nm against the ibuprofen concentration. Samples were drawn from the release medium at predetermined intervals and returned to the release vessel after measurement of the absorbance. All drug-release tests were carried out six times to control the homogeneity, and the results obtained from the samples were averaged. In some experiments, Sörensen's medium was renewed every 24 h to discern whether equilibrium conditions were reached during release.

Release models

The release rates were calculated from the experimental results by the following theoretical models.

First-order model[58,59]

$$\ln(1 - M_t/M_0) = -k_1 t \tag{2}$$

where M_t is the amount of drug released at time t, k_1 is the first-order release constant, and M_0 is the total amount of drug in the sample. In this case, the drug released at each time was proportional to the residual drug inside the dosage form.

Higuchi square root of time model:[60,61]

$$M_t M_0 = k_H t^{1/2} \tag{3}$$

where k_H is the Higuchi release constant. This is the most widely used model to describe drug release from a homogeneous planar matrix with the assumption that the dosage form does not dissolve.

The combination of the Higuchi and first-order models described the first (0–60%) and last part of the release (40–100%), respectively. In this case, the equations[62] were derived for films of uniform thickness (l). The equations allowed a diffusion coefficient (D) to be determined.

Early time approximation

$$M_t/M_0 = k_H t^{1/2} [0 \le M_t/M_0 \le 0.6; k_H = 4(D/\pi l^2)^{1/2}] \tag{4}$$

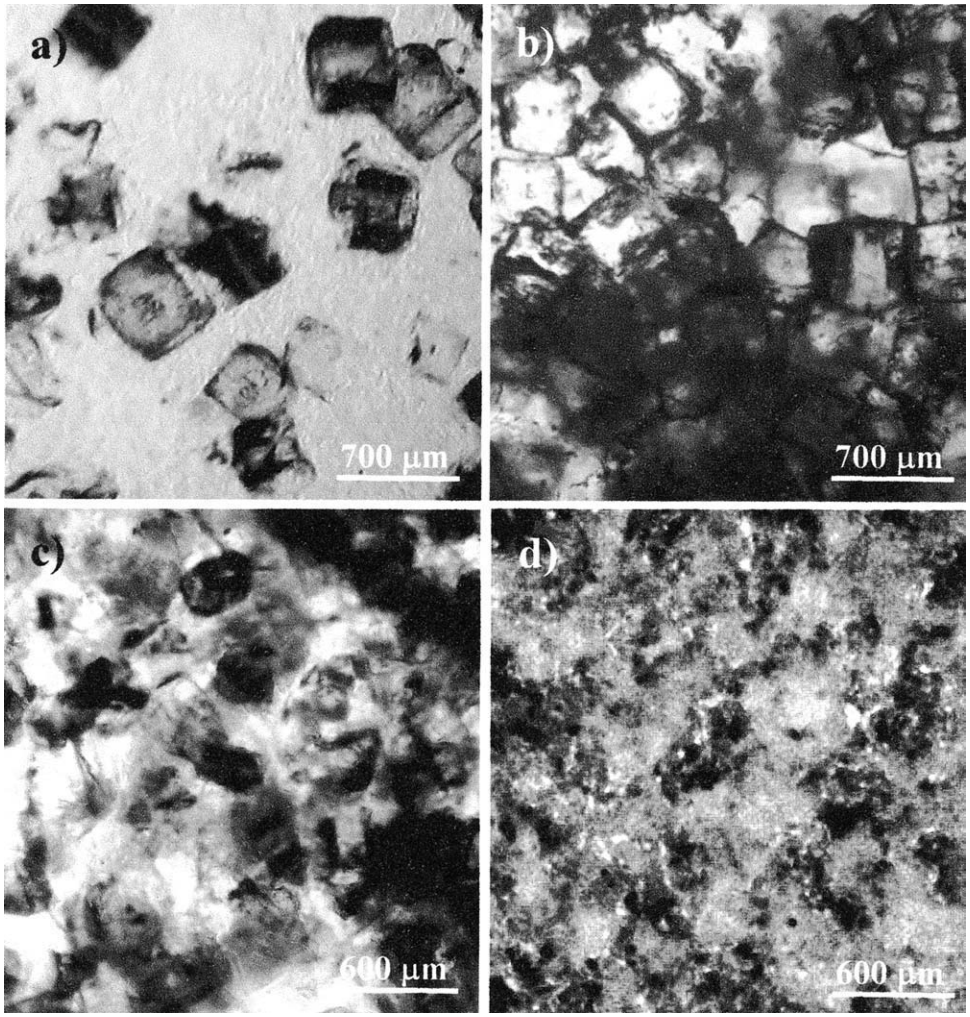

Figure 1 Optical micrographs of samples containing (a) 75 wt % PADAS and 25 wt % NaCl, (b) 50 wt % PADAS and 50 wt % NaCl, (c) 50 wt % PADAS and 50 wt % NaCl, and (d) 50 wt % PADAS and 50 wt % NH_4HCO_3. Salt particles have sizes of (a) 500-250, (b) 500-250, (c) 250-100, and (d) 250-100 μm.

Late-time approximation

$$\ln(1 - M_t/M_0) = 8/\pi^2 - k_1 t (0.4 \leq M_t/M_0 \leq 1.0; k_1 = \pi^2 D/l^2) \quad (5)$$

RESULTS AND DISCUSSION

Porous structure of the PADAS scaffolds

PADAS scaffolds were prepared by the compression-molding/particulate-leaching technique. NaCl and NH_4HCO_3 were selected as the porogen compounds, and two fractions of different particle sizes (LS and BS) were considered. The concentration of inorganic salt particles necessary to achieve an interconnected porous structure was first envisaged by optical microscopy, whereas the final characterization was performed by SEM and even by mercury intrusion porosimetry. Optical micrographs clearly showed that inorganic salt weight percentages lower than 50% resulted in a considerable ratio of isolated particles, which should have led to a decrease in the interconnective pores in the final scaffold. A homogeneous contact between granules was only detected at a higher salt concentration [e.g., see Fig. 1(a,b)]. Surface contact between the particles was greater for a given concentration when the low size fraction was employed [e.g., see Figs. 1(b,c)] because of its more efficient packing. The distribution of salt particles was clearly observed in the optical micrographs when the highly regular cubic NaCl crystals were used, unlike when the more irregular NH_4HCO_3 particles were employed [Fig. 1(d)]. Particle shape was also an important factor because interconnectivity between pores was expected to be enhanced for a given concentration when particles tended toward a spherical shape; this was also due to its more efficient packing. Note that cubic salt

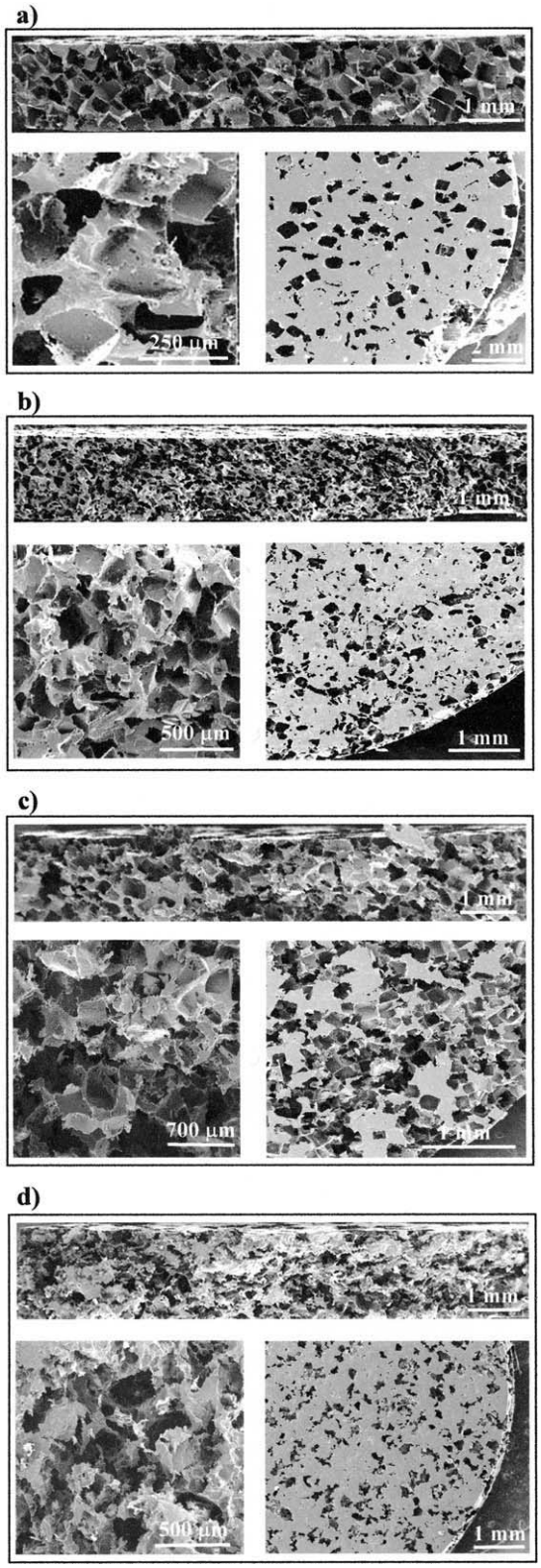

Figure 2 SEM micrographs of porous scaffolds fabricated from PADAS samples with an initial weight percentage of inorganic salt of (a,b) 70, (c) 80, and (d) 60%. Scaffolds were obtained with (a–c) NaCl and (d) NH_4HCO_3 salts of (a,d) big and (b,c) small particle size. Upper micrographs correspond to surface fractures, whereas lower micrographs show details of the porous structure inside the scaffold (left) and on the top disk surface (right).

particles have different ways to connect to each other, and consequently, the distribution of interconnectivity resulting from salt particles must have been, in this case, quite broad.

Scanning electron micrographs of the cross sections of salt-leached scaffolds (Fig. 2) clearly revealed a morphology characterized by a homogeneous distribution of pores inside the disk when a high concentration of salt was employed (i.e., >60%). High-magnification images showed the pore dimensions, interconnectivity, and wall thicknesses, which depended on the size and shape of the salt particles, as shown in Figure 2 for some representative preparations. The pores became more irregular, surrounded by thinner walls, and interconnected by larger openings as the porogen fraction increased and the particle size diminished, as can be shown in Figure 2(a,c). The top surface micrographs indicate the presence of a small number of pores on the disk surfaces, even when high salt concentrations were used.

The estimated porosity from the density measures clearly increased with the salt percentage and generally showed a slight increase when more irregularly shaped and smaller particles were employed, as qualitatively observed in the electron micrographs. Thus, for a 60% salt ratio, the porosity increased from 48 to 50% (NaCl particles) and from 54 to 58% (NH_4HCO_3 particles) when the LS fraction was used instead of the BS fraction, whereas for a 70% salt ratio, the values changed from 55 to 59% (NaCl particles) and from 63 to 67% (NH_4HCO_3). The effect of the particle size was not highly significant because of the small change in the estimated porosity percentages.

Figure 3 compares the pore size distribution, as obtained by mercury intrusion porosimetry, for representative scaffolds. Broader distributions with two populations of pores were then clearly observed when the bigger fraction of salt particles was used. The average diameter of pores decreased from 85 to 72 μm when the size of NaCl-leached particles diminished (i.e., BS vs LS fraction). The porosity values were comparable with those calculated from the density data. Thus, porosities of 46 and 56% were determined for the scaffolds prepared with 60 and 70%, respectively, of the BS fraction of NaCl particles.

Materials with porosities higher than 60% were too brittle, and therefore, subsequent studies were conducted with scaffolds prepared with 50–60 wt % inorganic salt only.

Crystallinity of the PADAS samples

The degree of crystallinity of a polymer matrix has a strong influence on the properties, especially the degradability and capability of favoring molecular diffusion. It was shown that PADAS had a complex

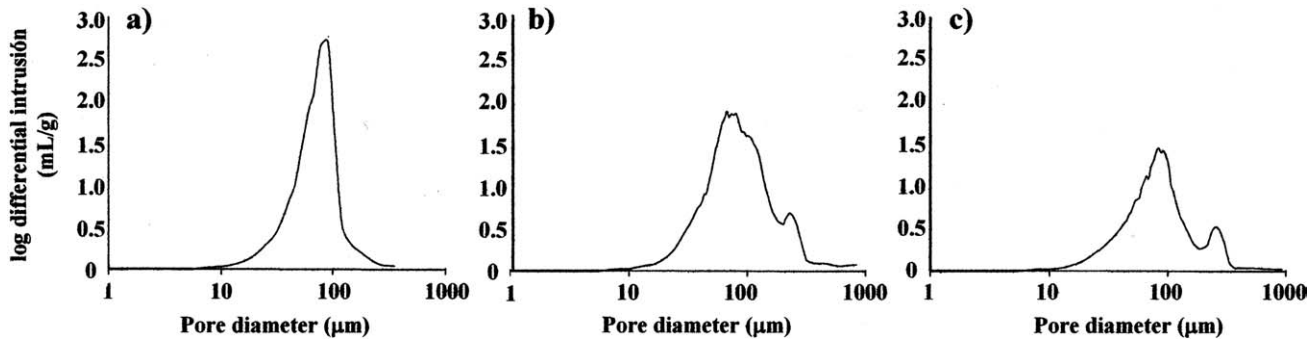

Figure 3 Porosimetric curves of scaffolds prepared from PADAS samples with an initial NaCl weight percentage of (a,b) 70 and (c) 60%. The particle sizes were (b,c) big or (a) small.

melting behavior, which depended on the preparation method and that a single X-ray fiber diffraction pattern was always attained.[55]

The polymer coming directly from synthesis showed three main melting peaks [[120 (T_1), 99 (T_2) and 89 °C (T3); Fig. 4(a)]; Fig. 4(a)], which could be associated with crystals of different lamellar thicknesses, according to previous observations.[55] It should be pointed out that a high melting enthalpy was measured (66 J/g) in contrast with the enthalpy of the exothermic peak (74°C) detected in a subsequent cooling run [Fig. 4(g)]. Thus, PADAS hardly crystallized from the melt state (with a recovery of crystallinity of 55%). The calorimetric heating trace of a PADAS sample pressed at 105°C [Fig. 4(b)] was different from the initial one because of the occurrence of a melt/recrystallization process. Note that the low-temperature melting peak observed at 89°C disappeared, whereas the intensity of the peak around 101°C increased. In this way, the more defective lamellae partially crystallized into thicker crystals. The total heat of fusion (52 J/g) was lower than that measured for the initial sample (66 J/g) because of the incompleteness of the recrystallization process.

The calorimetric behavior of pressed disks containing ibuprofen is shown in Figures 4(c) (17% ibuprofen) and 4(d) (28% ibuprofen). In the first case, three melting peaks were detected at temperatures lower than for the neat polymer, and a significant decrease in the global melting enthalpy was measured. This suggests the incorporation of some ibuprofen molecules into the crystalline domains also hindered crystallization. The second sample showed a greater decrease in the melting temperature of the representative peaks (see also Table I), which could have been related to a higher ibuprofen content. It is worth mentioning that this sample was pressed at only 80°C, and consequently, the melt/recrystallization process, and even the decrease in melting enthalpy, should have been less significant.

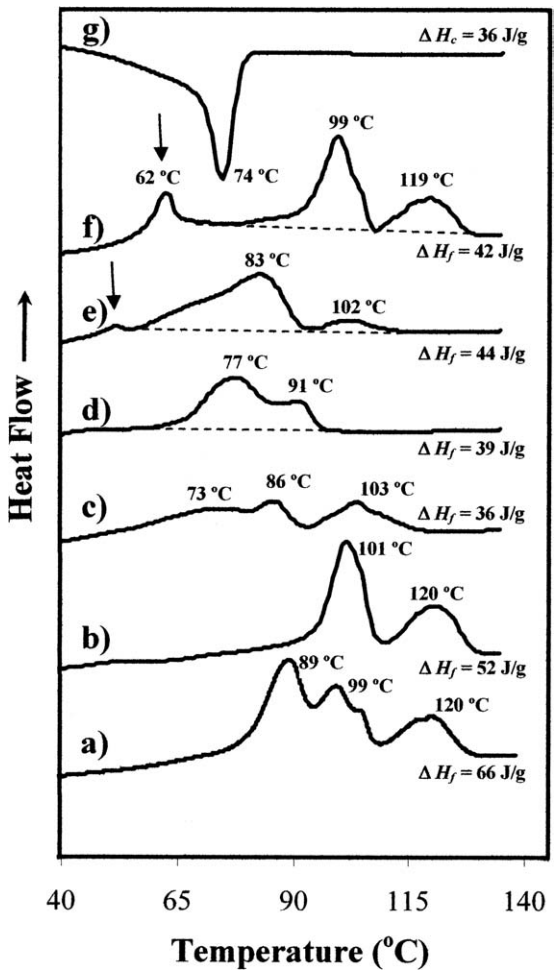

Figure 4 DSC heating runs of (a) PADAS coming directly from synthesis, (b) a PADAS disk pressed at 105°C for 15 min, (c) a PADAS disk containing 17% ibuprofen, (d) a PADAS disk containing 28% ibuprofen, (3) a PADAS scaffold prepared with 60 wt % NaCl and an initial ibuprofen load (before washing) of 23%, and (f) a PADAS scaffold prepared with 60 wt % NH_4HCO_3 and an initial ibuprofen load (before washing) of 23%. The percentages always refer to the mixture of PADAS and the specific component. (g) DSC cooling run of a melted PADAS sample coming directly from synthesis. Enthalpies always refer to the weight of PADAS, and measures were, therefore, corrected with consideration of the percentage of loaded ibuprofen. δH_f : Melting enthalpy; δH_c : Crystallization enthalpy.

TABLE I
Calorimetric Data and Degree of Crystallinity Determined by X-Ray Diffraction of Representative PADAS Samples

Sample	Pressing temperature (°C)	Ibuprofen content (wt %)	T_1 (°C)	T_2 (°C)	T_3 (°C)	δH_f (J/g)	X_c^{WAXD} (%)
Powder from synthesis	—	—	120	99–104	89	66	42
Powder from synthesis	105	—	120	101	—	52	37
NH_4HCO_3 scaffold[a]	25	10.9	119	99	—	42	33
NaCl scaffold[b]	80	15.3	102	83	77	44	24
Disk	105	17	103	86	73	36	27
Disk	80	28	91	77	—	39	31

[a] An additional peak was observed at 62°C.
[b] An additional peak was observed at 50°C.

Figure 4(e) corresponds to a scaffold prepared from NaCl particles and containing 15.3% ibuprofen. A strong similarity with the disk containing 17% ibuprofen [Fig. 4(c)] was found. Finally, Figure 4(f) shows the trace of the scaffold prepared from NH_4HCO_3 and containing 10.9% ibuprofen. In this case, two peaks associated with the neat polymer [note the resemblance with the trace in Fig. 4(b)], together with a new endothermic peak at 62°C, were detected. The latter may have corresponded to the fusion of impure ibuprofen crystals, which theoretically melt at 72°C. A similar peak (see solid arrows) could also be envisaged in the scaffold prepared from NaCl.

Table I summarizes the main calorimetric data of the previous representative samples. It must be pointed out that the ibuprofen molecules seemed to be well mixed in the PADAS matrix, except for the scaffold prepared from NH_4HCO_3 particles, which was pressed at only 25°C.

The relative crystallinities of the samples were determined by deconvolution of the corresponding WAXD patterns. Despite the complex melting behavior observed in the DSC heating traces, the diffraction patterns were highly similar, as expected for a single crystalline structure (Fig. 5). Thus, two amorphous halos centered at 0.437 and 0.363 nm were always observed, together with four Bragg reflections at 0.483, 0.461, 0.415, and 0.393 nm, with the strongest reflection appearing at 0.415 nm, as previously reported.[55] The ratio between the intensity of these Bragg reflections and the total intensity of the Bragg and amorphous reflections gave relative crystallinities (Xc^{WAXD}) between 24 and 42% (Table I). The sample coming directly from synthesis had the highest crystallinity, as also shown in Figure 5, where the relative intensity of its amorphous halos was lower than that determined for the scaffold samples. It should be pointed out that close agreement was generally found between the variation in the melting enthalpy and the WAXD crystallinity for all of the studied samples (Table I). Furthermore, crystallinities evaluated from calorimetric data by the group contribution theory also indicated a similar range[55] (e.g., 36 and 28% were estimated for the sample coming from synthesis and a melt-pressed sample, respectively). Finally, it was interesting to

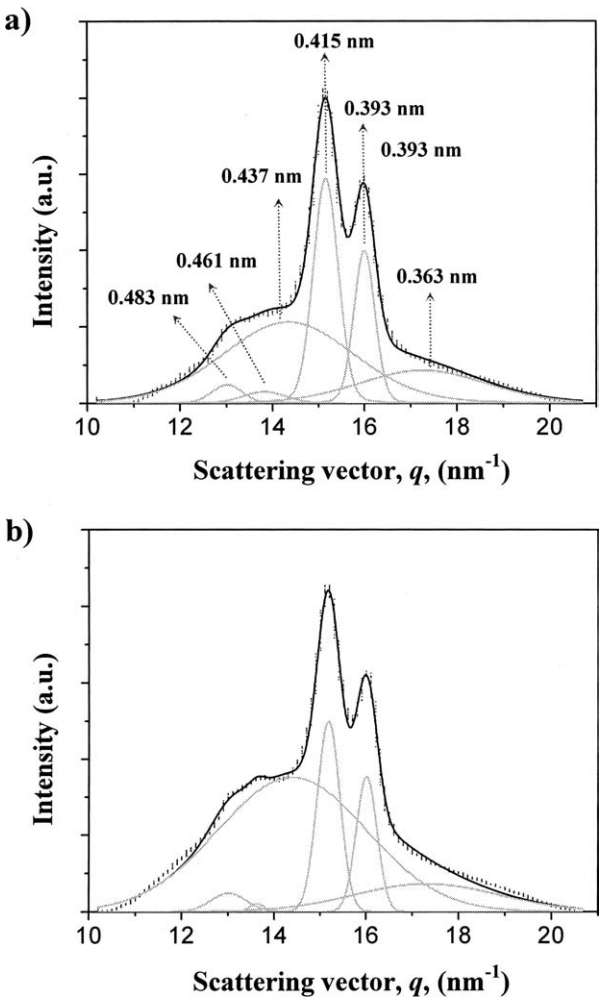

Figure 5 X-ray diffraction profiles [$q = (4\pi/\lambda) \times \sin\theta = 2\pi/d_B$], where dB is the Bragg spacing corresponding to (a) PADAS coming directly from synthesis and (b) a PADAS scaffold prepared with 60 wt % NaCl and an initial ibuprofen load (before washing) of 23 or 15.3% (after washing). Deconvoluted amorphous halos and crystalline peaks of the profiles corresponding to the polymer samples are indicated, together with the corresponding simulated profile (solid lines). The percentages always refer to the mixture of PADAS and the specific component.

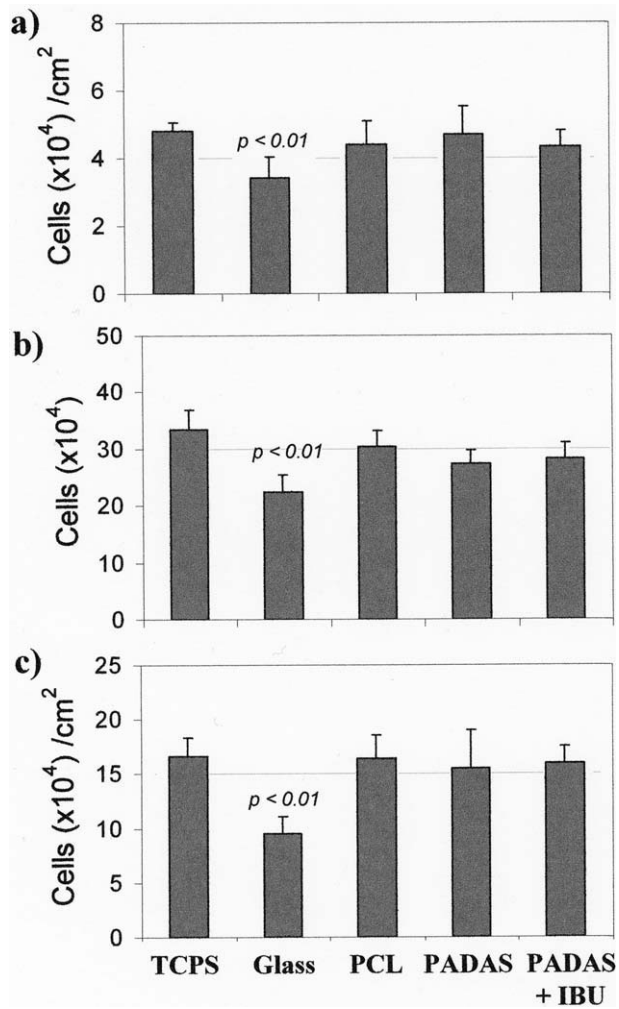

Figure 6 Adhesion and proliferation of MDCK cells on ibuprofen loaded and unloaded PADAS scaffolds: (a) attachment of MDCK cells to the surface of the indicated materials after 24 h of culturing, (b) cell viability (cells grown on the indicated material and around it) after 7 days of culturing, and (c) cell proliferation on the indicated materials after 7 days of culturing. The bars are the Mean ± Standard deviation; $p < 0.01$ versus the TCPS control, via Student t test IBU: Ibuprofen.

note that no reflections associated with ibuprofen crystals were detected in the diffraction patterns of the ibuprofen-loaded samples, except in the case of the scaffolds prepared from NH_4HCO_3 particles; this suggested that drug molecules were well dispersed in the polymer matrices when the samples were processed at temperatures close to the polymer melting temperature.

Cell adhesion and proliferation over the ibuprofen-loaded scaffolds

The *in vitro* biocompatibility of the new PADAS scaffolds was evaluated because of their potential and promising biotechnological applications, especially in biomedicine. In fact, poly(ester amide)s are a new emergent family of biocompatible materials, as revealed by several studies on cytotoxicity, cell adhesion, and cell proliferation (e.g., polymers derived from glycolic acid and ω-amino acid units[63]).

The attachment of MDCK cells to TCPS, cover glass (Thermanox), scaffolds from PCL microfibers, and ibuprofen-loaded and unloaded PADAS scaffolds is compared in Figure 6(a). After 24 h of culturing, significantly fewer MDCK cells were attached to the cover glass ($p < 0.01$) than to TCPS or PCL, which are standard supports for cell attachment, and the electrospun PCL scaffolds had a tridimensional porous texture, which may have mimicked the extracellular matrix composed of fibrillar proteins (e.g., collagen).[64] It should be pointed out that results indicate that PADAS scaffolds loaded with 9 wt % ibuprofen and unloaded PADAS scaffolds facilitated cell adhesion at a similar ratio to that observed for the TCPS and PCL supports. In this way, the cell adhesion to PADAS surfaces suggests good *in vitro* biocompatibility during cell–polymer interaction. The ability of PADAS to support cell adhesion might be related to its chemical structure, whose hydrophobic character, conferred by its long polymethylenic segments, can be compensated by the presence of highly hydrophilic amide groups. Thus, the considerable amount of surface energy associated with hydrophilic groups may have influenced or favored cell adhesion to PADAS scaffolds. The attachment of MDCK cells is an early event that determines the subsequent success in the proliferation and colonization of the material.

The viability of MDCK cells after 7 days of seeding on PADAS scaffolds can be seen in Figure 6(b). The result clearly shows that PADAS had no cytotoxic effects on cells adhered to the material and around it. MDCK cells were seeded at a density of 2×10^4 cells/well (30% confluence), and after 7 days of culture, they reached a density of 3×10^5 cells/well (90% confluence). This study also reveals that in comparison to TCPS and PCL [Fig. 6(c)], PADAS scaffolds supported cell growth with high levels of cell viability.

The decrease of cellular viability depends on the concentration of released ibuprofen. Thus, ibuprofen at 10^{-2} *M* reduced the cellular viability at 60–90% in a culture of normal human fibroblasts. Concentrations of ibuprofen of 10^{-4} and 10^{-3} *M* have been reported as capable of significantly decreasing the response *in vitro* to proinflammatory stimulators. In these cases, cultures show high levels of cellular viability (>90%).[65] In this way, one of the implications of this work is that any initial burst release of ibuprofen from the scaffolds (as described later) did not appear to be high enough to adversely affect the cellular viability to any significant degree. Approximately, the maximum release of ibuprofen from a

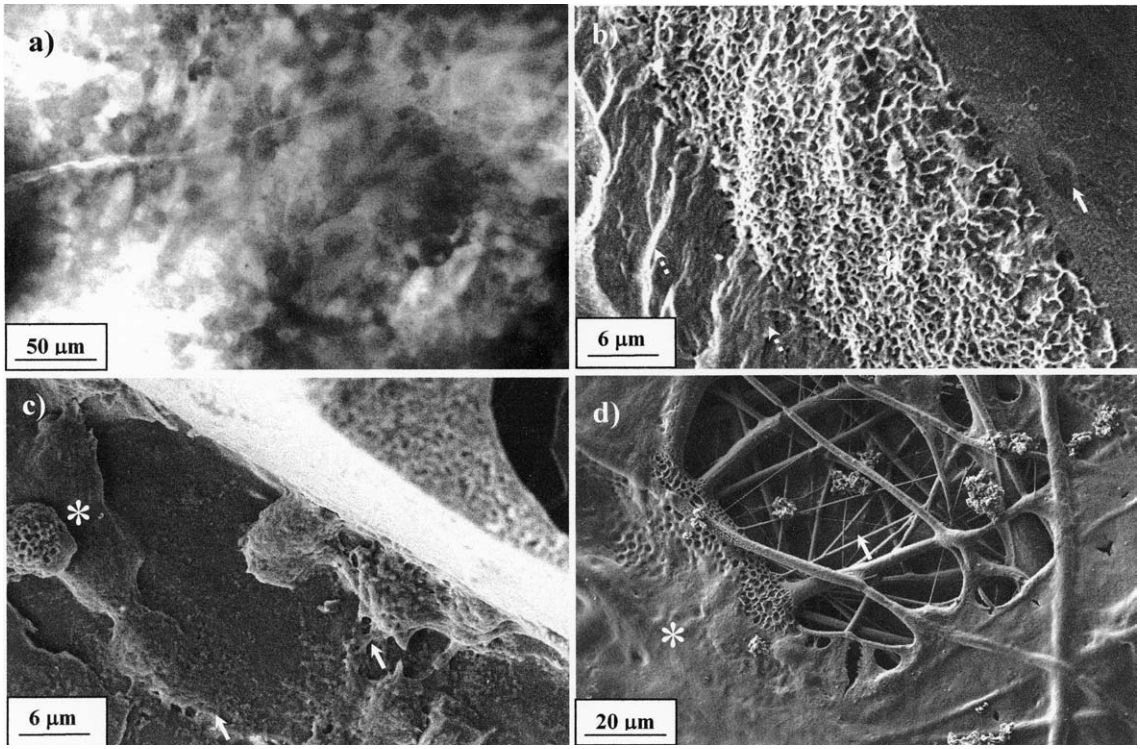

Figure 7 Morphology of MDCK cells cultured on scaffolds for 7 days. (a) Optical micrograph of a cell monolayer spread uniformly on the PADAS material surface. (b) SEM image showing the cell monolayer spread over (solid arrow) and into (dashed arrows) the PADAS scaffold. The micrograph also shows a rough fracture surface where the noncolonized material is also visible (asterisk). (c) SEM image of cells in the pore of an ibuprofen-loaded PADAS scaffold. Evidences of the cellular colonization can be observed (arrows indicate the cytoplasm extensions showing spreading, and the asterisk indicates a monolayer cell array). (d) SEM image of cells over the PCL scaffold control (the arrow indicates the PCL microfibers, and the asterisk indicates the cell monolayer).

disk of PADAS into 1 mL of media over 24 h gave a concentration of 10^{-4} *M* [see Fig. 8(b), shown later]. Thus, this explains the high viability of cells in the presence of the PADAS scaffolds loaded with ibuprofen.

Figure 7 shows the morphology of MDCK cells after 7 days of culturing on the PADAS scaffolds. Cell spreading and good attachment to the polymer surface was observed. More interestingly, cells were organized in a uniform monolayer like a cellular tissue [Figs. 7(a,b)] and could also be found in the inner scaffold pores [Fig. 7(c)]. Thus, both loaded and unloaded PADAS scaffolds supported cell growth and allowed complete colonization of the material. For the sake of completeness, an SEM image of cells grown into the PCL positive control is also shown in Figure 7(d).

In vitro culture systems for epithelial cells can be used to study different aspects of cell attachment, growth, and differentiation. The epithelial cell morphology of apical and basal regions is different and gives rise to so-called polarized cells. Epithelial cells cultured on a tridimensional matrix can form large disorganized colonies when this membrane polarity is lost. In our case, the observed monolayer growth suggested that no differentiation changes occurred.

Ibuprofen release from the compact PADAS disks

Figure 8(a) shows the release profiles of ibuprofen in Sörensen's medium at 37°C from disks containing different weight percentages of the drug (9–28%). The thickness of the disks varied between 1125 and 1430 μm, depending on the amount of incorporated ibuprofen. Release first occurred by diffusion of the drug through the polymer matrix, which was defined by *D*, and then by a mass transfer between the boundary layer of the sample and the release medium. The experimental results clearly show that delivery was significantly faster when the percentage of loaded ibuprofen increased, despite the increase in disk thickness and presumably longer diffusion path for the ibuprofen molecules. In all cases, the ibuprofen content was totally delivered into the Sörensen's medium because of the hydrophilic character and good solubility in aqueous media of the drug. For the sake of completeness, some experiments were performed by renewal of the

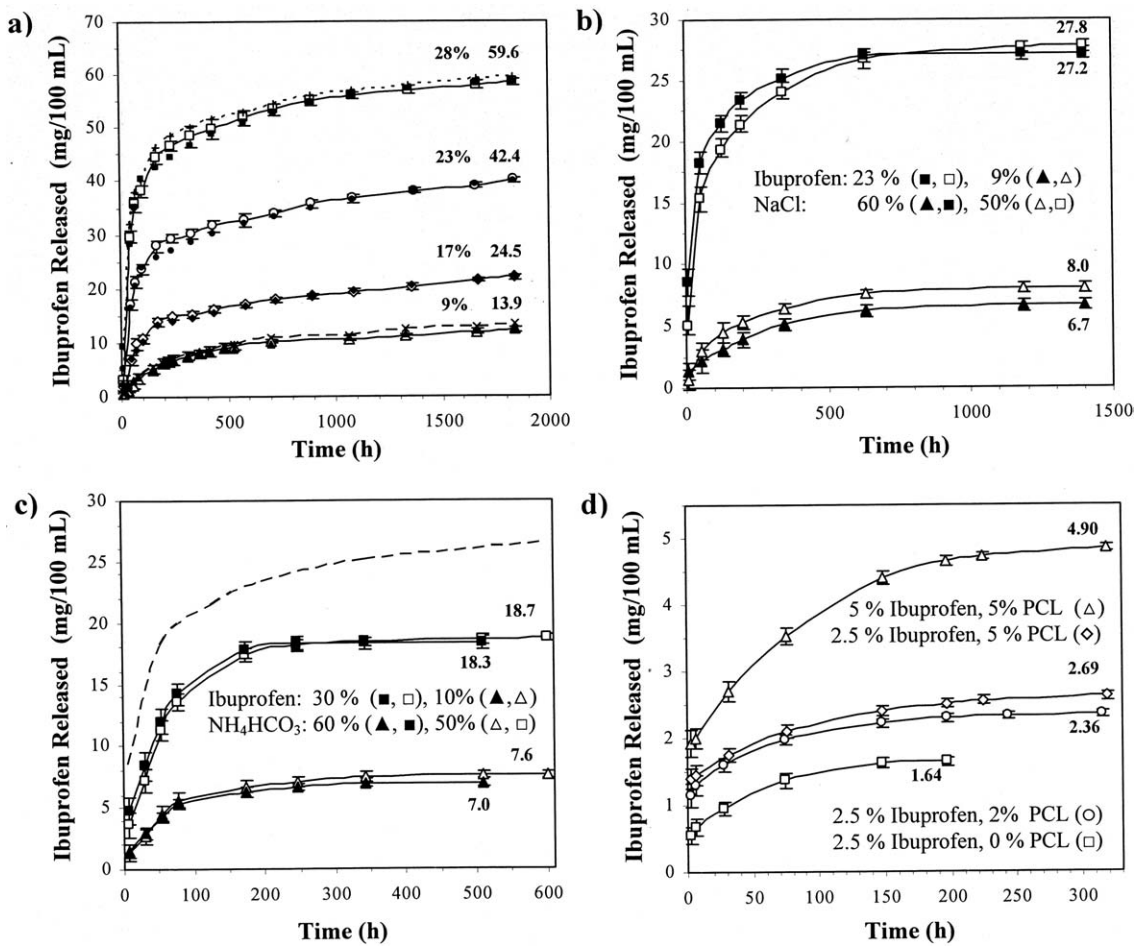

Figure 8 Release of ibuprofen in Sörensen's medium at 37°C from different samples. In all cases, the maximum concentration corresponding to the total release of ibuprofen incorporated is indicated in the profiles of each ibuprofen content: (a) PADAS disk samples containing the indicated ibuprofen weight percentages. Release was performed with (dashed lines) and without (solid lines) medium renewal. Theoretical release data deduced by application of the combined Higuchi/first-order model are shown by full symbols. (b) Porous scaffolds prepared with the indicated percentages of small-size NaCl particles and containing the indicated ibuprofen weight percentages. (c) Porous scaffolds prepared with the indicated percentages of small-size NH_4HCO_3 particles and containing the indicated ibuprofen weight percentages. For the sake of completeness, the release profile of a scaffold prepared with 60% small-size NaCl particles and 30 wt % ibuprofen is also shown (dashed line). (d) Porous scaffolds loaded by immersion in ethyl acetate solutions containing the indicated weight-to-volume percentages of ibuprofen and PCL.

release medium every 24 h. The profiles were practically identical to those attained under static conditions [Fig. 8(a)], although the release rate was obviously slightly higher. Initially, all of the release curves showed a rapid process where 50 to 70% of the drug was delivered in a short period of 200 h, followed by a slow, sustained delivery that could cover a period of 1900 h.

TABLE II
Correlation Coefficients, Release Rate Constants, and *D* Values for the Ibuprofen Release of PADAS Disks in a Sörensen's Medium at 37°C as Deduced with Different Mathematical Models

		Model									
		First-order		Higuchi		Early time approximation			Late-time approximation		
Ibuprofen (wt %)	Disk thickness (μm)	r	k_1 (h^{-1})	r	k_H ($h^{-0.5}$)	r	k_H ($h^{-0.5}$)	D (m^2/s)	r	k_1 (h^{-1})	D (m^2/s)
9	1125	0.872	0.0014	0.923	0.025	0.985	0.030	6.29×10^{-14}	0.985	0.0009	3.21×10^{-14}
17	1230	0.796	0.0014	0.782	0.025	0.979	0.042	1.45×10^{-13}	0.988	0.0009	3.83×10^{-14}
23	1330	0.755	0.0018	0.539	0.028	0.976	0.057	3.13×10^{-13}	0.984	0.0011	5.47×10^{-14}
28	1430	0.812	0.0025	0.402	0.030	0.967	0.070	5.38×10^{-13}	0.989	0.0017	9.78×10^{-14}

r is the correslation coefficient.

Table II clearly indicates that the best agreement for the release process was obtained with the combined model. This gave high correlation coefficients at the beginning (0.97–0.99) and in the last stage (0.98–0.99) of the release. Figure 8(a) also plots the simulated release data obtained with the combined model and the corresponding release constants to graphically show the goodness of the fit with the experimental curves.

The calculated D values (Table II) were similar for the last stage of the release and especially when the ibuprofen load was low (e.g., 3.21–3.83 $\times$ 10^{-14} m^2/s). Reasonable agreement was found even between coefficients deduced from the first and last release stages for the lowest ibuprofen load of 9% (6.29 $\times$ 10^{-14} vs 3.21 $\times$ 10^{-14} m^2/s). However, the D values sharply increased (e.g., 5.38 $\times$ 10^{-13} m^2/s) with the ibuprofen load during the first release stage; this indicated that at high concentrations, the ibuprofen molecules were not well trapped in the polymer matrix. The D values of a similar magnitude order were determined for the ibuprofen release from poly(ε-caprolactone-*co*-D,L-lactide)[66] and poly(*p*-dioxanone)[67] loaded with 5% of the drug (i.e., 1.5 $\times$ 10^{-13} and 3.9 $\times$ 10^{-13} m^2/s). In any case, it should be pointed out that results suggested a higher molecular interaction when the poly(ester amide) was employed instead of the indicated polyesters. Thus, the hydrophobic character conferred by the long polymethylenic sequences of PADAS could be compensated by the presence of highly hydrophilic amide groups.

Ibuprofen release from the scaffolds loaded before salt leaching

Figure 8(b) shows the release profiles of ibuprofen in Sörensen's medium at 37°C from scaffolds prepared with NaCl particles (LS fraction with weight percentages of 60 and 50%) and different initial weight percentages of the drug (9 and 23%). The salt-leaching process resulted in a highly significant ibuprofen release, and consequently, the ibuprofen content of the scaffold sample decreased, as deduced from the final weight of the scaffold and the amount of PADAS incorporated into the disk. Thus, values of 5.1–4.3% and 15.6–15.3% were determined for samples with initial ibuprofen percentages of 9 and 23%, respectively. A slightly larger decrease after salt leaching was logically detected when the sample had a porous structure (i.e., when salt percentages of 60% were used). It should be pointed out that ibuprofen percentages of 7.3 and 15.4% could be predicted with the previously deduced mathematical model for compact disk samples after 48 h of exposure to the release medium and initial ibuprofen percentages of 9 and 23%, respectively. The results were highly comparable, although differences induced by

TABLE III
Correlation Coefficients and Release Rate Constants for Fitting to the Combined Mathematical Model of the Ibuprofen Release Profiles of PADAS Scaffolds (Prepared from Small-Size NaCl or NH_4HCO_3 Particles) in a Sörensen's Medium at 37°C

NaCl (wt %)[a]	Ibuprofen (wt %)[a]	Ibuprofen loaded (mg/disk)	Early time approximation		Late-time approximation		NH_4HCO_3 (wt %)[a]	Ibuprofen (wt %)[a]	Ibuprofen loaded (mg/disk)	Early time approximation		Late-time approximation	
			r	k_H ($h^{-0.5}$)	r	k_1 (h^{-1})				r	k_H ($h^{-0.5}$)	r	k_1 (h^{-1})
50	9	8.0	0.992	0.065	0.993	0.0034	50	9	7.6	0.979	0.079	0.989	0.0117
60	9	6.7	0.999	0.075	0.996	0.0044	60	9	7.0	0.994	0.084	0.967	0.0266
50	23	27.8	0.998	0.075	0.998	0.0038	50	23	18.7	0.990	0.080	0.993	0.0100
60	23	27.2	0.961	0.095	0.971	0.0047	60	23	18.3	0.991	0.088	0.963	0.0350

r is the correslation coefficient.

porosity appeared enhanced when the ibuprofen load was low (i.e., values of 9, 5.1, and 4.3% were deduced for samples prepared with the low ibuprofen load and 0, 50, and 60% salt, respectively, whereas values of 23, 15.6, and 15.3% were deduced for related samples with the high ibuprofen load).

The experimental release data fit well with the combined model (Table III), although the relevance of the early time approximation was low for samples with an initial small ibuprofen load because of the delivery of a great drug percentage during the salt-leaching process. The data summarized in Tables II and III clearly showed the increase in the release constants with increased porosity for both steps. These changes were a direct consequence of the shorter diffusion path for ibuprofen molecules with porosity. With regard to the experimental release curves, drug delivery occurred over a long time period of approximately 700 h, which increased with decreasing porosity (i.e., 1800 h for compact disks).

Noticeably different behavior was observed when the scaffolds were prepared with the NH_4HCO_3 porogen agent. In this case, a large ibuprofen percentage was liberated during the elimination of the inorganic salt. Thus, the remaining ibuprofen content decreased to 4.8–4.4 and 11–10.9% for initial loads of 9 and 23%, respectively, when the disks were exposed to the aqueous medium at 45°C for only 2 h. Higher ibuprofen percentages (i.e., 8.7 and 21.6%) were calculated for compact disk samples exposed to the release medium for the same period of time and the same initial ibuprofen load. The results clearly suggest a significant burst effect, which could have been a consequence of the low pressing temperature used to prepare disks and which led to a bad mixture of drug and polymer matrix.

Figure 8(c) shows the ibuprofen release profiles in Sörensen's medium at 37°C from scaffolds prepared with NH_4HCO_3 particles (LS fraction with weight percentages of 60 and 50%) and the indicated ibuprofen load percentages. The release data fit well again with the combined model (Table III), with the release constants being higher than those calculated for similar scaffolds prepared with NaCl particles. Thus, the release was almost complete after a shorter period (i.e., 300 vs 700 h). The data in Table III show small differences between samples during the first release step. However, the estimated constants for the late-time approximation increased significantly with porosity (i.e., from 0.01 to 0.035 h^{-1} for scaffolds prepared with 50 and 60% NH_4HCO_3 particles). Note that the effect of the initial ibuprofen load was small and that the first-order release constants were higher in one magnitude order despite a lower ibuprofen content than those calculated for the NaCl scaffolds (i.e., 0.035 and 0.0047 h^{-1} for samples prepared with 60% inorganic salt). This seemed to prove again that ibuprofen molecules were less trapped in the PADAS matrix when disk pressing was performed at a low temperature.

Ibuprofen release from the scaffolds loaded by immersion

A second procedure for loading the drug was immersion of the scaffold in an ethyl acetate solution containing a given concentration of ibuprofen (5 and 2.5% w/v). Scaffolds were prepared with 60% NaCl particles (LS fraction). In this case, ibuprofen was basically deposited over the large internal surface areas of the scaffold, and consequently, a rapid release was expected. PCL was also added (2 and 5% w/v) to the immersion bath to cover the scaffold internal surfaces with a polymeric film, which should have been able to trap ibuprofen molecules and delay drug delivery.

Figure 8(d) contains the release profiles of the studied samples. In all cases, the amount of loaded ibuprofen was small, as deduced from the ibuprofen concentration measured at the end of the release process. This load logically increased with the concentration of PCL in the ethyl acetate solution (i.e., the weight percentages varied from 1.6 to 4.9 mg/disk when PCL was increased from 0 to 5% w/v). Release curves fit well with a first-order model and showed a burst effect (Table IV), which was indicative of the existence of some molecules adhered to the external surfaces only. However, it was interesting to note that the release extended over a significant time interval (200–320 h), even when PCL was not used; this means that ethyl acetate could swell

TABLE IV
Correlation Coefficients and Release Rate Constants for the Ibuprofen Release of PADAS Scaffolds (Prepared by the Immersion Method) in a Sörensen's Medium at 37°C as Deduced with a First-Order Model

Immersion bath		Ibuprofen loaded (mg/disk)	Ibuprofen released burst effect (mg/disk)	First-order model	
PCL (wt %)	Ibuprofen (wt %)			r	k_1 (h^{-1})
0	2.5	1.64	0.30	0.988	0.027
2	2.5	2.36	1.14	0.999	0.015
5	2.5	2.69	1.33	0.999	0.012
5	5	4.90	1.61	0.999	0.013

r is the correslation coefficient.

the polymer matrix and facilitate drug diffusion inside it. Note that release was studied in Sörensen's medium, which has no swelling effect to facilitate diffusion. Thus, a significant difference was found between the immersion time (2 h) and the total release time (200 h when PCL was not employed). The release constants logically decreased (Table IV) with the concentration of PCL, and for a given PCL content, they increased with the amount of loaded ibuprofen. It is worth pointing out that the main change was observed between samples prepared with and without PCL (i.e., 0.027 and 0.015 h^{-1}). The calculated constants were of a similar magnitude order to those found in the rapid release described previously for scaffolds prepared from NH_4HCO_3 particles (Table III).

CONCLUSIONS

Scaffolds based on a poly(ester amide) matrix (PADAS) derived from a natural amino acid such as L-alanine could be prepared with appropriate porosity, good thermal properties, and mechanical consistence by the compression-molding/particulate-leaching technique. These characteristics were attained with NaCl particles with sizes between 250 and 100 μm and with a weight percentage close to 60%

Scaffolds of PADAS were not cytotoxic, supported cell growth, and showed good cell viability. Biocompatibility results were comparable to standard materials such as PCL. The grown cells were predominantly confluent, and consequently, the polymer substrate could not induce morphological modifications.

Hydrophobic PADAS scaffolds showed a sustained release of a hydrophilic drug, ibuprofen, without producing a negative effect on the cell viability. Drug release was highly dependent on the loading method (i.e., direct mixture of components before processing or immersion of scaffolds in solutions containing the drug) and could be extended over a period of nearly 2000 h. In the first case, the release kinetics in a Sörensen's solution was generally well described with a combined model based on two steps that followed the Higuchi equation at the beginning and a first-order equation at the end of the delivery process. The model allowed the estimation of the D values, which ranged between 3×10^{-14} and 5×10^{-13} m^2/s. In the second case, a significant burst effect was found; this was due to the existence of molecules adhered to the external surfaces. The addition of PCL to the immersion loading bath diminished this burst effect and increased the release period because of its coating effect.

The reported results demonstrate the suitability of PADAS, a hydrophobic polymer of the emerging group of biodegradable poly(ester amide)s derived from natural amino acids, to be used as a scaffold matrix. PADAS allowed the sustained release of a hydrophilic drugs, ibuprofen, that could be controlled by variation of the loading method.

References

1. Langer, R.; Vacanti, J. P. Science 1993, 260, 920.
2. Hayashi, T. Prog Polym Sci 1994, 19, 663.
3. Thomson, R. C.; Wake, M. C.; Yaszemski, M.; Mikos, A. G. Adv Polym Sci 1995, 122, 247.
4. Pachence, J. M.; Kohn, J. Principles of Tissue Engineering; Lanza, R. P.; Langer, R.; Vacanti, J. P., Eds.; Academic: New York, 1997; p 273.
5. Kim, B. S.; Mooney, D. Trends Biotechnol 1998, 16, 224.
6. Langer, R. J Controlled Release 1999, 62, 7.
7. Chapekar, M. S. J Biomed Mater Res Part B: Appl Biomater 2000, 53, 617.
8. Holland, T. A.; Mikos, A. G. Adv Biochem Eng Biotechnol 2006, 102, 161.
9. Jagur-Grodzinski, J. Polym Adv Technol 2006, 17, 395.
10. Martina, M.; Hutmacher, D. W. Polym Int 2007, 56, 145.
11. Hollister, S. J. Adv Mater 2009, 21, 3330.
12. Langer, R. Adv Mater 2009, 21, 3235.
13. Freed, L. E.; Vunjak-Novakovic, G. Adv Drug Delivery Rev 1998, 33, 15.
14. Kim, B. S.; Mooney, D. J. Trends Biotechnol 1998, 16, 224.
15. Salgado, A. J.; Coutinho, O. P.; Reis, R. L. Macromol Biosci 2004, 4, 743.
16. Sachlos, E.; Czernuszka, J. T. Eur Cells Mater 2003, 5, 29.
17. Sokolsky-Papkova, M.; Agashi, K.; Olaye, A.; Shakesheffb, K.; Domb, A. J. Adv Drug Delivery Rev 2007, 59, 187.
18. Thomson, R. C.; Yaszemski, M. J.; Powers, J. M.; Mikos, A. G. Biomaterials 1998, 12, 1935.
19. Shastri, V. P.; Martin, I.; Langer, R. Proc Natl Acad Sci USA 2000, 97, 1970.
20. Hassan, C.; Peppas, N. Adv Polym Sci 2000, 153, 37.
21. Sundback, C. A.; Shyu, J. Y.; Wang, Y. D.; Faquin, W. C.; Langer, R. S.; Vacanti, J. P.; Hadlock, T. A. Biomaterials 2005, 26, 5454.
22. Nam, Y. S.; Yoon, J. J.; Park, T. G. J Biomed Mater Res Part B: Appl Biomater 2000, 53, 1.
23. Nam, Y. S.; Yoon, J. J.; Park, T. G. J Biomed Mater Res Part B: Appl Biomater 2000, 53, 1.
24. Nazarov, R.; Jin, H. J.; Kaplan, D. L. Biomacromolecules 2004, 5, 718.
25. Kanczler, J. M.; Barry, J.; Ginty, P.; Howdle, S. M.; Shakesheff, K. M.; Oreffo, R. O. C. Biochem Biophys Res Commun 2007, 352, 135.
26. Whang, K.; Thomas, C. H.; Healy, K. E.; Nuber, G. Polymer 1995, 36, 837.
27. Lo, H.; Ponticiello, M. S.; Leong, K. W. Tissue Eng 1995, 1, 15.
28. Zhang, K.; Wang, Y.; Hillmyer, M. A.; Francis, L. F. Biomaterials 2004, 25, 2489.
29. Nam, Y. S.; Park, T. G. J Biomed Mater Res 1999, 47, 8.
30. Freed, L. E.; Marquis, J. C.; Nohria, A.; Emmanual, J.; Mikos, A. G.; Langer, R. J Biomed Mater Res 1993, 27, 11.
31. Lu, H. H.; El-Amin, S. F.; Scott, K. D.; Laurencin, C. T. J Biomed Mater Res Part A 2003, 64, 465.
32. Li, W. J.; Laurencin, C. T.; Caterson, E. J.; Tuan, R. S.; Ko, F. K. J Biomed Mater Res 2002, 60, 613.
33. Yoshimoto, H.; Shin, Y. M.; Terai, H.; Vacanti, J. P. Biomaterials 2003, 24, 2077.
34. Jabbari, E.; Wang, S.; Lu, L.; Gruetzmacher, J. A.; Ameenuddin, S.; Hefferan, T. E.; Currier, B. L.; Windebank, A. J.; Yaszemski, M. J. Biomacromolecules 2005, 6, 2503.

35. Lam, C. X. F.; Mo, X. M.; Teoh, S. H.; Hutmacher, D. W. Mater Sci Eng C 2002, 20, 49.
36. Corry, D.; Moran, J. Biomaterials 1998, 19, 1295.
37. Cooper, S. A. Am J Med 1984, 77, 70.
38. Slavic-Svircev, V.; Heidrich, G.; Kaiko, R. F.; Rusy, B. F. Am J Med 1984, 77, 84.
39. Bostrom, A. A.; Forbes, J. A.; Adoflsson, C.; Beaver, W. T.; Bell, W. E. Pharmacotherapy 1994, 14, 305.
40. Romsing, J.; Walther-Larsen, S. Anaesthesia 1997, 52, 673.
41. Mortera, R.; Onida, B.; Fiorilli, S.; Cauda, V.; Vitale-Brovarone, C.; Baino, F.; Vernè, E. Chem Eng J 2007, 137, 54.
42. Agrawal, C. M.; Athanasiou, K. A.; Heckman, J. D. Mater Sci Forum 1997, 250, 115.
43. Hutmacher, D. W. Biomaterials 2000, 21, 2529.
44. Middleton, J. C.; Tipton, A. J. Biomaterials 2000, 21, 2335.
45. Ryner, M.; Albertsson, A. C. Biomacromolecules 2002, 3, 601.
46. Jung, Y.; Kim, S. H.; You, H. J.; Kim, Y. H.; Min, B. G. J Biomater Sci Polym Ed 2008, 19, 1073.
47. Benedetti, L.; Cortivo, R.; Berti, T.; Berti, A.; Pea, F.; Mazzo, M.; Moras, M.; Abatangelo, G. Biomaterials 1993, 14, 1154.
48. Okada, M. Prog Polym Sci 2002, 27, 87.
49. Lips, P. A. M.; Dijkstra, P. J. Biodegradable Polymers for Industrials Applications; CRC: Boca Raton, FL, 2005; Chapter 5, p 198.
50. Rodríguez-Galán, A.; Franco, L.; Puiggalí, J. Polymers 2011, 3, 65.
51. Horwitz, J. A.; Shum, K. M.; Bodle, J. C.; Deng, M. X.; Chu, C. C.; Reinhart-King, C. A. J Biomed Mater Res 2010, 95, 371.
52. Bettinger, C. J.; Bruggeman, J. P.; Borenstein, J. T.; Langer, R. S. Biomaterials 2008, 29, 2315.
53. Gomurashvili, Z. D.; Katsarava, R.; Chumburdze, G.; Mumladze, N.; Tugushi, D. U.S. Pat. 0253809 A1 (2009).
54. Lips, P. A. M.; Dijkstra, P. J. Biodegradable Polymers for Industrials Applications; CRC: Boca Raton, FL, 2005; Chapter 5, p 198.
55. Paredes, N.; Rodríguez-Galán, A.; Puiggalí, J.; Peraire, C. J Appl Polym Sci 1998, 69, 1537.
56. Rodríguez-Galán, A.; Pelfort, M.; Aceituno, J. E.; Puiggalí, J. J Appl Polym Sci 1999, 74, 2312.
57. Vera, M.; Puiggalí, J.; Coudane, J. J Microencap 2006, 23, 686.
58. Gibaldi, M.; Feldman, S. J Pharm Sci 1967, 56, 1238.
59. Wagner, J. G. J Pharm Sci 1969, 58, 1253.
60. Higuchi, T. J Pharm Sci 1961, 50, 874.
61. Higuchi, T. J Pharm Sci 1963, 52, 1145.
62. Baker, R. Controlled Release of Biologically Active Agents; Wiley: New York, 1987; Chapter 4.
63. del Valle, L. J.; Sepulcre, F.; Gámez, A.; Rodríguez-Galán, A.; Puiggalí, J. Curr Trends Polym Sci 2008, 12, 27.
64. Ma, Z. W.; Kotaki, M.; Inai, R.; Ramakrishna, S. Tissue Eng 2005, 11, 101.
65. Cantón, I.; McKean, R.; Charnley, M.; Blackwood, K. A.; Fiorica, C.; Ryan, A. J.; MacNeil, S. Biotechnol Bioeng 2010, 105, 396.
66. Ahola, N.; Rich, J.; Karjalainen, T.; Seppälä, J. J Appl Polym Sci 2003, 88, 1279.
67. Zurita, R.; Puiggalí, J.; Rodríguez-Galán, A. Macromol Biosci 2006, 6, 767.